Fine Scale Structures in the RTP Tokamak Plasma, Measured with High Resolution Thomson Scattering

LOPES CARDOZO Niek*, DE BAAR Marco, BARTH Rolie, BEURSKENS Marc,
GORINI Giuseppe[1,2], HOGEWEIJ Dick, KARELSE Frank, MANTICA Paola[1],
VAN DER MEIDEN Hennie and SCHILHAM Arnold

*FOM-Instituut voor Plasmafysica 'Rijnhuizen', Associatie Euratom-FOM, Trilateral Euregio Cluster
P.O. Box 1207, NL 3430 BE Nieuwegein, the Netherlands;*

[1] *Istituto di Fisica del Plasma 'P. Caldirola', Associazione Euratom-ENEA-CNR, Milano, Italy*

[2] *INFM and Dip. di Fisica 'G. Occhialini', Università degli Studi di Milano-Bicocca, Milano, Italy*

Abstract

The Rijnhuizen Tokamak RTP, closed in Sept.1998, was unique for its combination of dominant 2nd harmonic ECH (4–7 times the Ohmic power, deposited within 10% of the minor radius) and high-resolution electron diagnostics. By scanning the ECH deposition through the plasma, electron transport barriers associated with the rational q-values 1, 4/3, 3/2, 2, 5/2, and 3 were experimentally demonstrated. Modulated ECH showed that the transport barriers are layers of strong inward convection. The ECH power is deposited just outside the barriers. A conceptual model was developed in which transport barriers are linked to rational q-values. The model reproduces all of the essential features of the RTP data sets, and was also tested against data from JET and TEXTOR.

Keywords:

1. Introduction

Anomalous transport of heat and particles remains one of the most intriguing puzzles in thermonuclear research. In recent years experimental conditions have been identified in which the heat transport by the ions is, at least in transient states, reduced to the neo-classical level (e.g. [1]). The reduction is generally attributed to suppression of micro-instabilities by sheared $E \times B$ flow. In the same conditions, the electron heat transport remains anomalous. It thus appears to be governed by a different mechanism, with magnetic turbulence as an important candidate.

The research programme of the Rijnhuizen Tokamak Project (RTP) focused on electron transport phenomena. Emphasis was placed on the possible role of small-scale (magnetic) structures in the plasma: transport barriers, magnetic islands, etc. The tokamak RTP ($R = 0.72$ m, $a = 0.16$ m, $B_T < 2.5$ T, $I_p < 150$ kA, pulse length ≈ 0.5 s, boronised vessel) was equipped with 2nd harmonic electron cyclotron heating (ECH: 500 kW, 110 GHz 2nd harm. X-mode, injected from the low field side) and high-resolution electron diagnostics. The ECH power could exceed the total Ohmic dissipation by a factor of 4 (for off-axis heating) to 7 (for central heating), and could be localised to within 10% of the minor radius. The diagnostic park included a 19 channel interferometer, and a 20 channel heterodyne ECE

Corresponding author's e-mail: cardozo@rijnh.nl

system as well as a 16 channel ECE-Imaging diagnostic (imaging a vertical chord), both operating in 2nd harm. X-mode. For highest spatial resolution, a double pulse Thomson scattering measurement of the full radial profiles of the electron temperature and density (T_e and n_e) with a spatial resolution of < 3 mm was available.

The aim of the present paper is to bring together in a concise form evidence for a radial fine structure of electron heat transport. The detailed description of the experiments is scattered over a number of papers, many of which have already been published, while some are very recent or not yet published. Here we summarise this large body of experimental data and the interpretation and modelling results, and discuss this in the context of work done in other groups.

In Sec. **2** we present evidence for electron thermal transport barriers. The evidence results partly from experiments in which the radial position at which the ECH power is deposited was scanned with 1 mm steps, and partly from inspection of measured T_e-profiles in discharges with off-axis ECH. In this way 6 electron thermal barriers could be identified.

In Sec. **3** we show that the barriers are associated with simple rational values of q (at the position of the barrier), namely 1, 4/3, 3/2, 2, 5/2, and 3. This identification is based on the occurrence of MHD-modes (off-axis sawteeth), and on reconstructed q-profiles.

Based on these experimental results, a conceptual transport model was constructed. This model is based on the single assumption that the electron thermal diffusivity (χ_e) is a function of q only, with transport barriers near simple rational values of q. This model was tested against data from RTP, TEXTOR and JET and found to perform well (Sec. **4**).

In the discussion, the observations are placed in the context of recent publications of related work in other groups.

2. Experimental Evidence for Electron Thermal Transport Barriers

Series of experiments were carried out in which the ECH deposition radius ($\rho_{dep} = r_{dep}/a$) was varied between 0 and ≈ 0.6 with steps of < 0.01 (1 mm in the plasma!). Deposition at $\rho_{dep} > 0.6$ suffered from bad single pass absorption. In all cases reported in this paper, the deposition was on the low field side of the magnetic axis. The deposition radius was varied by tuning the toroidal magnetic field. Figure 1 shows a set of T_e-profiles measured with Thomson scattering, for 5 values of ρ_{dep}. In all cases, the measurements were taken

> 150 ms ($\approx$ 100 energy confinement times and 10 current diffusion times) after ECH was switched on. At this time all diagnostics indicated that the plasma has reached a thermal equilibrium.

The generic features are very peaked profiles for central deposition, and profiles that are flat or even hollow inside ρ_{dep} for off-axis ECH. Outside ρ_{dep} the profiles are very similar. Papers dealing with the different profile shapes and the transitions between them are found under [2-4].

In RTP off-axis ECH generally results in hollow T_e-profiles. A power balance analysis showed that radiation losses and the electron-ion energy exchange cannot account for the reversed gradients [4,5]. Thus, a convective heat flux must be invoked to explain the profiles obtained with off-axis ECH. We return to this subject after presenting evidence for convection in transport barriers in RTP. This result is in apparent contradiction with the observation of peaked T_e-profiles in DIII-D under off-axis ECH [6], but a recent re-evaluation of the power deposition in that experiment resolves this conflict [7].
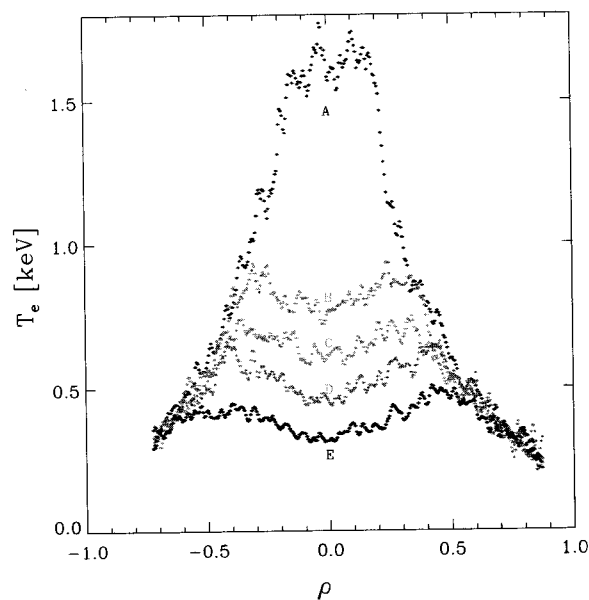
Fig.1 Profiles of the electron temperature of EC-heated plasmas, measured with high resolution Thomson scattering. The profiles are measured well into a steady state period. For central ECH peaked profiles are observed. For off-axis ECH, steady state hollow profiles are obtained. Outside the ECH deposition the profiles are all very similar.
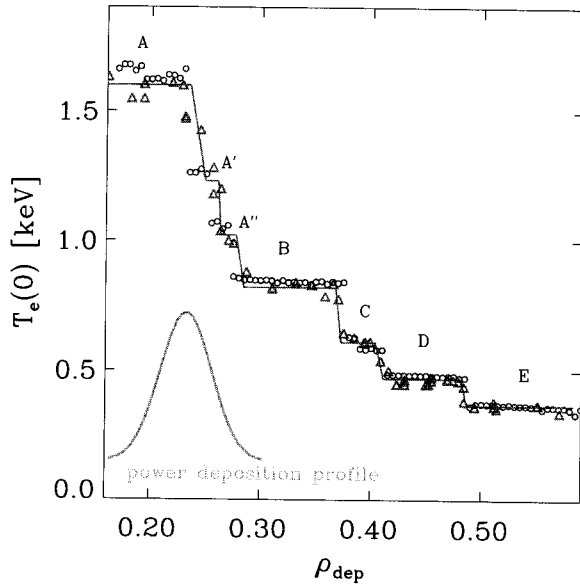
Fig. 2 A shot-to-shot scan of the ECH deposition radius revealed step-wise changes of the electron temperature profile. Five main levels of $T_e(0)$ were identified, and two sub-levels between A and B. The triangles are data points, the line is drawn to guide the eye. Also shown are the results of a simulation (circles) with a transport model featuring transport barriers near simple rational q values (Sec. 4).

Fig. 3 A comparison of T_e-profiles at either side of the e.g. B-C transition (i.e. with nearly the same ρ_{dep}) reveal that the transition is due to the loss of a narrow region of steep gradient, i.e. a transport barrier. Apart from this barrier the profiles are almost identical.

The basic result on transport barriers is contained in very detailed scans of the ECH deposition radius, obtained in series of discharges with near identical conditions. Figure 2 shows the result of such a scan. Clearly, there is a stair-step relationship between ρ_{dep} and $T_e(0)$, with sharp transitions separating plateaux (labelled A-E) in which $T_e(0)$ is insensitive to a variation of ρ_{dep}. The subdivision of the A-B transition in two intermediate levels is based on additional information: discharges are observed to make spontaneous transitions between A, B and the two intermediate levels, as measured with ECE (see [2,4]).

Comparing T_e-profiles on either side of a transition shows that the difference is due to a narrow region where the 'high $T_e(0)$' discharge has a steep gradient, which is absent in the 'low $T_e(0)$' discharge. An example is given in Fig. 3. Apart from this region of steep gradient the profiles are very similar, both in the central region and in the wings. We shall refer to such regions of steep T_e-gradient as transport barriers.
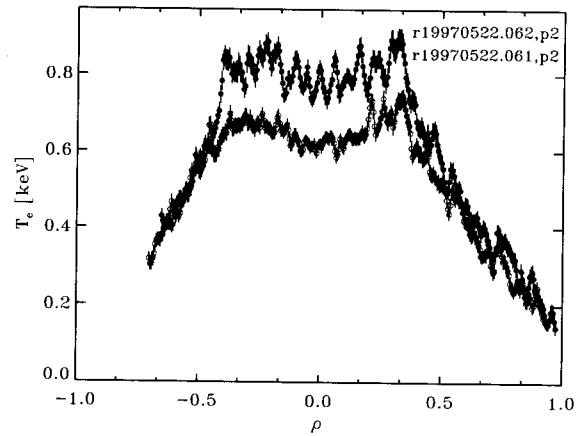
It should be remarked that to demonstrate the presence of electron transport barriers directly, i.e. as features of the T_e-profile, requires that the second derivative of T_e be measured with a spatial resolution of $\approx 2\%$ of the minor radius and good accuracy. This is at the limit of even the high resolution Thomson scattering diagnostic at RTP.

Having demonstrated the presence of electron transport barriers, we devised experiments to investigate the heat transport in the barriers by means of modulated ECH. The propagation of the temperature perturbations was followed by ECE. Careful analysis of the phase and amplitude data at several harmonics of the modulation frequency revealed that the barriers are layers of strong inward heat convection [8]. The same analysis revealed that the ECH deposition is at the foot of the barriers, i.e. just outside rather than inside.

Summarising, the scan of ρ_{dep} shows sharp transitions of the T_e-profile, for specific values of ρ_{dep}. The transitions are much sharper than the width of the ECH deposition. A transition is due to the loss of a transport barrier. Transport in the barriers is dominated by inward heat convection.

3. Experimental Evidence that links the Barriers to Simple Rational q-values

The barriers can be linked to values of q through the occurrence of MHD-modes. Off-axis sawtooth activity (see [9] for a detailed account) occurs for ρ_{dep}

close to, but smaller than a transition value. Through analysis of the dominant oscillation at the crash time, the mode structure of these MHD modes could be determined. This links the transitions A''-B, B-C, and D-E to $q = 3/2$, 2 and 3, respectively. (Sawteeth at the C-D transition have been observed, but the quality of the data did not allow a mode analysis).

This picture is corroborated by q-profiles computed from the measured T_e-profile and additional information, using neo-classical resistivity and correcting for the bootstrap current. This analysis is only done for discharges that have been in thermal equilibrium for several current diffusion times, and that do not show MHD activity. Typical results for the 5 main levels are given in Fig. 4. Note that for the 5 levels the minimum q values separate out in 5 bands of half-integer q. Independent measurements of the current density using tangential Thomson scattering - which are only available for a restricted data set - corroborate this conclusion [10].
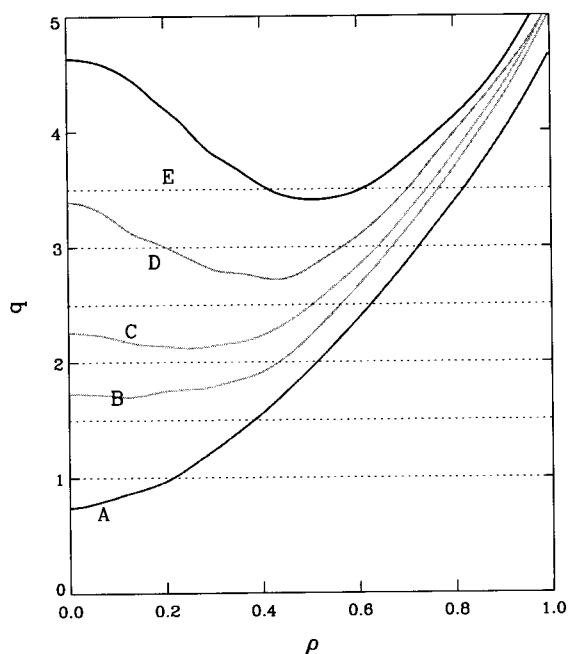
4. A Conceptual Transport Model

Based on the experimental findings, a transport model was constructed with the following properties [11]:

- The electron thermal diffusivity χ_e shows an alternation of transport barriers and region of high conduction.
- The transport barriers are linked to the local value of q, and that is the only functional dependence in the model.
- The width of the barriers, expressed in a range of q, is chosen the same for all barriers (0.08). The depth of the barriers is determined in a procedure to match the experimental data.
- The value of χ_e in the layers between the barriers is chosen the same.

The model is implemented in a time dependent transport code, in which also the evolution of the current density profile is computed. This is necessary, because the q profile determines the χ_e-profile, so that energy and current diffusion must be solved self-consistently.

Figure 5 shows χ_e as function of q as it was used in the code. With this function, keeping all parameters fixed except ρ_{dep}, the phenomenology of the experimental ρ_{dep} scan was very successfully simulated (see Fig. 2).

Fig. 4 *q*-profiles of typical discharges in the 5 main levels (A-E, see Fig. 2), computed assuming neo-classical resistivity. The 5 levels correspond to 5 half integer *q*-bands. In a transition, qmin crosses a half integer value.
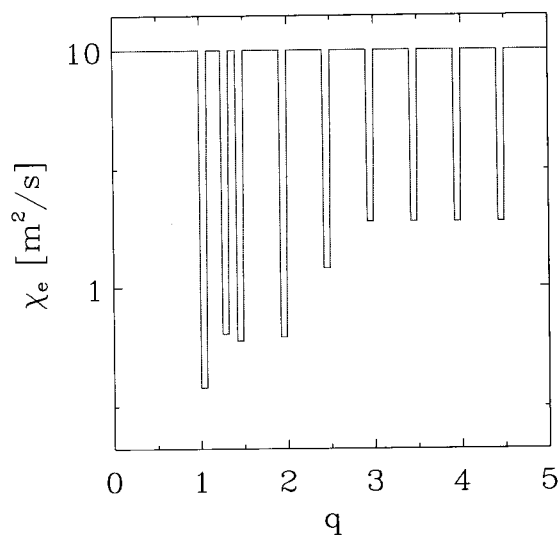

Fig. 5 The experimental data could be explained by invoking a heat diffusivity which is a function of *q* only, with transport barriers near simple rational values of *q*. Note that in this model the thermal resistance of a barrier depends on the local shear (see Fig. 6)

94

Note that the free parameters in the model basically allow a match for $T_e(0)$ in the plateaux, but not for the values of ρ_{dep} at which the transitions occur. Further, the model gives a good match of the T_e-profiles. Moreover, the striking observation that the transitions occur for a variation of ρ_{dep} much smaller than the ECH deposition region, is reproduced by the model. (It is a result of the non-linear interaction between the χ_e and q-profiles). Another salient aspect of the experimental data, i.e. the formation of pronounced off-axis maxima on T_e for specific values of ρ_{dep} (close to a transition), was also reproduced by the model. Figure 6 shows how the T_e-peaks come about. It also illustrates how a transport barrier can become wide in real space if q has a low shear region in a 'low χ_e band'.

The model was first tested against a data set of a ρ_{dep} scan in RTP, for a single set of plasma parameters [11]. After that, the model was tested against 6 data sets, in which the plasma current and n_e were varied [12]. (Note that a single data set typically contains 50–100 discharges). Further, the model was carried over to TEXTOR and tested against the first results obtained with ECH in that tokamak (see Fig.7). This simulation was obtained by taking the RTP model parameters and only apply a uniform scale factor according to L-mode scaling. No individual parameter fitting was applied to obtain the result in Fig. 7.

Finally, the model was applied to optimised shear discharges in JET, where it proved capable of predicting the time and location of barrier formation, as well as the evolution of the barrier (place and height). Here, the model parameters were tuned in the Ohmic phase of the discharge. With the parameters thus fixed, the evolution of the discharged was computed self-consistently using the JETTO code [13].

It should be pointed out that in this model the barriers are layers of reduced diffusivity, whereas the experiments with modulated ECH have shown that they are in fact layers of inward convection. The reason why we chose for 'diffusive' barriers in the model is that the number of free parameters becomes too large with convective barriers: when convection is introduced, there always remains a diffusive part of transport. To model both effectively doubles the number of free parameters. We note, however, that for steady state situations there is effectively no difference between 'convective' or 'diffusive' barriers. Likewise, one needs perturbative techniques to distinguish the two experimentally.

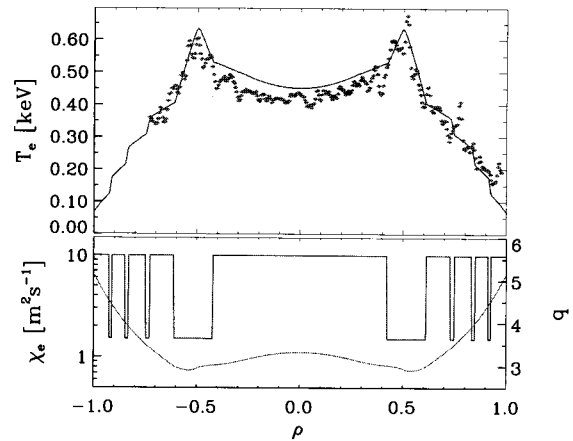We did try to run the model with convective barriers. The results confirmed the statements made above.

Fig. 6 Example of a simulation with the model presented in Fig. 5, compared to experimental data. The model gives a fair reproduction of the very pronounced 'ears' on the T_e-profile. Note that no parameters were tuned for this specific case: the parameters are the same as for the overall match to the ρ_{dep} scan (Fig. 2). The model does provide an explanation for the formation of the 'ears': the off-axis minimum of q falls in a low χ_e band, leading to a wide barrier.
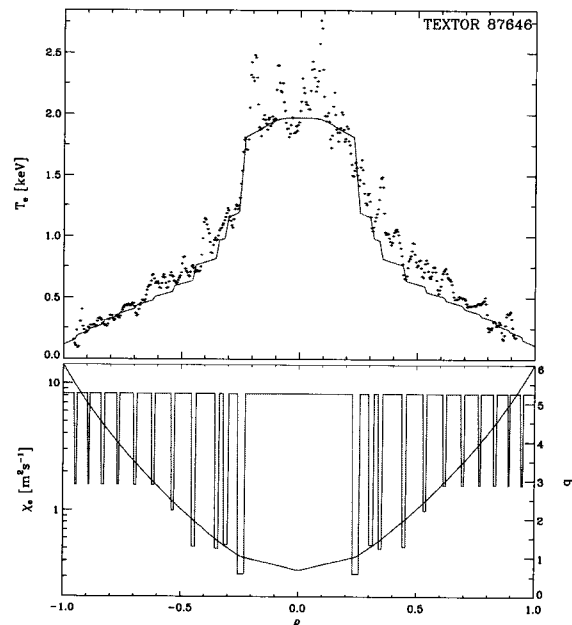

Fig. 7 The model that was developed on the basis of experimental data obtained in ECH discharges in RTP, was applied to ECH discharges in TEXTOR-94 by applying a single scaling factor (0.85) based on L-mode scaling to all χ-values. Without any further adjustments, this resulted in the match to the experimental profile shown.

95

So: yes, it is possible to recover the same quality of simulations, and second: yes, there is ambiguity in the parameters of the model: convection and conduction can be mixed and give rise to a range of equally good simulations.

In summary, we have modelled the barriers as regions of reduced diffusivity, whereas in fact they are regions of inward convection. Since the simulations concern steady plasma states, this is allowed. Of course, one should be careful to always realise that the transport barriers such as presented in Fig.5 may represent a layer of inward heat convection.

5. Discussion

The main thrust of the work presented in this paper is that the electron thermal transport is governed by the presence of transport barriers at simple rational q values. The fact that the barriers depend explicitly on q is sufficient to explain a range of peculiar observations with strong off-axis ECH. The same minimum set of assumptions proved to give useful predictions for limited data sets from TEXTOR and JET.

Let us first point out that the model is an interpretation of the data. The T_e profile transitions in the ρ_{dep} scan, and the associated high-resolution T_e profiles demonstrate the presence of only one barrier per transition. In the model, all barriers are always present, but only the one in a low shear region becomes clearly visible. Also the reverse is true: barriers in high shear regime are outside the accuracy of present measuring techniques. There is some evidence in the high-resolution profiles of a sequence of barriers similar to that in the model, but the evidence is not conclusive. Figure 8 gives an example of a comparison between the model (the standard form, no parameters were fitted for this particular profile) and the measured T_e profile, which do show similarity in the finer structures.

The barrier model shows that an alternating χ_e can describe a wide range of transport aspects with a minimum of assumption. It bears some resemblance to earlier (semi-empirical) transport models in which chains of islands play a role, such the 'venetian blind' model [14], the Rebut-Lallia-Watkins model [15], and work by Kadomtsev [16] and Gianakon et al [17].

An important consequence is that if electron heat transport is indeed governed by a sequence of barriers, a power balance analysis may give erratic results. A power balance analysis normally does not resolve the barriers and therefore yields the harmonic average of χ_e, which may be difficult to interpret. In particular, the
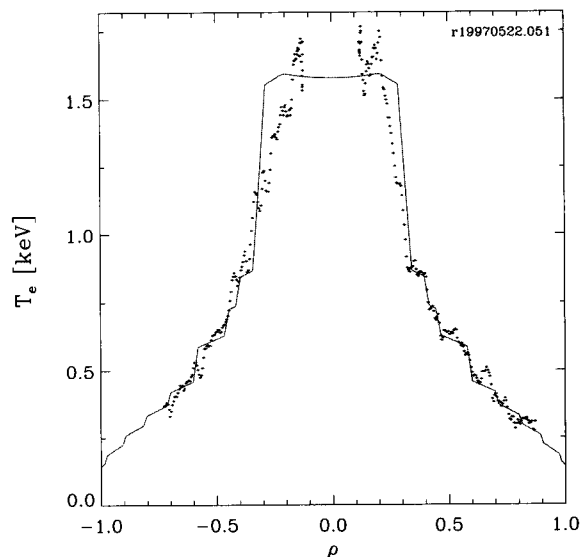

Fig. 8 Comparison of the χ_e profile in RTP as measured by Thomson scattering and predicted by the transport barrier model, for central ECH. Note that the sequence of barriers in the gradient zone give rise to only small 'steps' in the simulated profile. Such steps are difficult to demonstrate experimentally, even with the high resolution Thomson scattering T_e measurement available at RTP. Yet, the structure visible in the measured profile is well comparable to that in the simulated profile.

scaling of this average χ_e with plasma parameters will be a mix of the parametric dependencies of χ_e in the barriers and the conduction zones. Thus, different physical transport mechanisms are mixed in a single parameter. To unravel these dependencies, it is necessary to resolve the transport barriers.

Moreover, the barriers are convection dominated. This finding further compromises the local power balance analysis, which assumes purely diffusive transport. As a general conclusion, we believe that the results on electron transport presented in this paper show that a comparison between experimental results on electron heat transport and theoretical predictions must be carried out with extreme care. There is no experimental quantity that can readily be compared to a theoretical prediction of χ_e.

While for ion thermal transport barriers the relation to rational q values is widely believed to be weak at best, there is ample evidence for such a relation in the case of electron thermal transport barriers. The association of electron transport barriers to $q = 2$ was e.g.

reported from JET [18], while in JT-60 transport barriers near $q = 3$ were found [19]. Special mention should be made of T-10, in which experiments with ECH similar to those in RTP were carried out, with similar results [20].

It is well known that there is relation between energy confinement and the edge iota value in optimised stellarators [21]. This relation was recently recovered with an empirical transport model [22] that is very similar to the model presented in the present paper. In the stellarator model, transport is low everywhere except near rational surfaces, so that at first it appears to be the opposite of our model. However, since the density of rational numbers is lowest near the low order rational numbers, this model effectively has transport barriers centred at rational iota (or q) values.

The common element to such models is that the magnetic topology is determining the transport. Certainly, the magnetic topology lies at the basis of the observed structure. However, the precise mechanism is quite unclear. Again, from our experiments it appears that the barriers are convection dominated. Thus, models that simply postulate chains of islands and associated bad confinement do not do justice to the physics.

There may be much more complex reasons why electrons transport shows a structuring which reflects the magnetic topology. In [23] it is shown that transport reduction due to $E \times B$ shear flow may concentrate at rational q values. Also, Thyagaraja [24] finds such a structure in computational transport studies based on electro-magnetic modes. Recent results obtained by Thyagaraja with the 'CUTIE' code show striking similarity to the experimental data from RTP, including the formation of hollow profiles and 'ears'.

In summary, our experiments give food for the idea that the electron transport in a tokamak has a fine radial structure. This structure is a layering, where layers with high transport are alternated with layers of inward convection and good net insulation. The physical processes giving rise to this layering have not been isolated in the experiment. The magnetic topology plays an important role. Less clear is the role of electric fields and associated $E \times B$ flow shear. We believe that it is essential for further understanding of electron heat transport that this spatial structure is taken into account.

Acknowledgement

References

[1] C.M. Greenfield *et al.*, Phys. Plasmas **4**, 1596-1604 (1997).

[2] M. de Baar, G.M.D. Hogeweij, N.J. Lopes Cardozo, A.A.M. Oomens and F.C. Schüller, Phys Rev. Lett. **78**, 4573-4576 (1997).

[3] N.J. Lopes Cardozo *et al.*, Plasma Physics and Control. Fusion **39**, B303 (1997).

[4] M.R. de Baar, M.N.A. Beurskens, G.M.D. Hogeweij and N.J. Lopes Cardozo, Physics of Plasmas **6**, 4645-4657 (1999).

[5] G.M.D. Hogeweij *et al.*, Phys. Rev. Lett. **76**, 632-635 (1996).

[6] C.C. Petty and T.C. Luce, Nucl. Fusion **34**, 121-130 (1994).

[7] C.B. Forest, R.W. Harvey and A.P. Smirnov, Nucl. Fusion **41**, 619-623 (2001).

[8] P. Mantica, G. Gorini, G.M.D. Hogeweij, N.J. Lopes Cardozo and A.M.R. Schilham, Phys. Rev. Lett. **85**, 5434-5437 (2000).

[9] R.F.G. Meulenbroeks *et al.*, Physics of Plasmas **6**, 3898-3905 (1999).

[10] F.A. Karelse *et al.*, Plasma Phys. Control Fusion **43**, 1-26 (2001).

[11] G.M.D. Hogeweij, N.J. Lopes Cardozo, M.R. de Baar and A.M.R. Schilham, Nucl. Fusion **38**, 1881-1891 (1998).

[12] A.M.R. Schilham, G.M.D. Hogeweij and N.J. Lopes Cardozo, Electron thermal transport barriers in RTP: experiment and modelling, Plasma Phys. Control. Fusion **43**, 1699 (2001).

[13] A.M.R. Schilham, N.J. Lopes Cardozo, G.M.D. Hogeweij, V.Parail and C. Gormezano, Application of the RTP transport model to the JET tokamak, accepted for publication in Nuclear Fusion.

[14] R.R. Dominguez and R.E. Waltz, Nucl. Fusion **27**, 65 (1987).

[15] P.H. Rebut, M. Brusati, M. Hugon and P.P. Lallia, Proc. 11th International Conference on Plasma Physics and Controlled Nuclear Fusion Research, Kyoto, 1986 (IAEA, Vienna, 1987) Vol.2, p 187

[16] B.B. Kadomtsev, Plasma Transport in Tokamaks, Nucl. Fusion **31**, 1301 (1991).

[17] T.A. Gianakon, J.D. Callen and C.C. Hegna, Phys. Plasmas **1**, 2245-53 (1994).

[18] C. Gormezano *et al.*, Phys. Rev. Lett. **80**, 5544 (1998).

[19] Y. Koide *et al.*, Plasma Phys. Control. Fusion **38**, 1011 (1996).

[20] K.A. Razumova *et al.*, Plasma Phys. Control.

Fusion **42**, 973 (2000).

[21] Neuhauser *et al.*, rep. IPP 5/30 (1989) Max-Planck Institut für Plasmaphysik, Garching

[22] R.Brakel *et al.*, in Proc. 25th EPS Conf. on Control. Fusion and Plasma Physics, Prague (1998) Vol 22C, p423

[23] C. Hidalgo *et al.*, this conference; also C. Hidalgo *et al.*, Plasma Phys. Control. Fusion **42**, A153 (2000).

[24] A. Thyagaraja, Plasma Phys. Control. Fusion **42**, B255 (2000).